AEGC2019 Data to Discovery
Australasian Exploration Geoscience Conference
2-5 September 2019 • Perth, Western Australia
Incorporating the AIG, ASEG, PESA, and WABS

Fractures extraction and associated intensity maps from 3D VSP data

Eric Takam Takougang
Khalifa University
Abu Dhabi
Eric.takougang@ku.ac.ae

Mohammed Y. Ali
Khalifa University
Abu Dhabi
mohammed.ali@ku.ac.ae

Youcef Bouzidi
Khalifa University
Abu Dhabi
youcef.bouzidi@ku.ac.ae

Fateh Bouchaala
Khalifa University
Abu Dhabi
fateh.bouchaala@ku.ac.ae

Aala Mohamed
Khalifa University
Abu Dhabi
aala.mohamed@ku.ac.ae

Akmal A. Sultan
Khalifa University
Abu Dhabi
akmal.sultan@ku.ac.ae

SUMMARY

Fractures and faults were extracted from a reverse time migrated 3D Vertical Seismic Profile (VSP) data acquired over a carbonate reservoir offshore Abu Dhabi in the United Arab Emirates. A specific workflow was used for the extraction of fractures and faults. The workflow was based on data preconditioning (i.e. noise attenuation), semblance based seismic attributes, binary filtering, and clustering. A complex network of fractures was extracted. The dominant strike direction of the extracted fractures showed a good correlation with the dominant strike direction of interpreted fractures from FMI (Fullbore Formation Microimager) and core data at three reservoir zones. A known fault in the area was also detected. The extracted fracture network was then used to compute fracture intensity maps. Fracture intensity maps give indications of zones with high fracturing that may be associated with greater porosity and permeability.

Keywords: fractures, faults, VSP, attribute, workflow.

INTRODUCTION

3D Vertical Seismic Profile (VSP) data were acquired in an oilfield offshore Abu Dhabi in the United Arab Emirates. The purpose of the survey was to provide high resolution seismic images for reservoir characterizations which include faults and fractures studies, as well as estimates of anisotropy.

The field is structurally a large anticlinal with very gentle dips that was formed during Late Cretaceous and Neogene times (Hassan and Wada, 1981), and is dominated by carbonate rocks from Jurassic to recent (Alsharhan, 1989). Complex multi-set patterns of faults at reservoir level characterize the field. These include strike-slip, dip-slip and also cross-faults system that appears to emanate from basement and display a flower structure (Edwards et al., 2005). Most of these faults are located on the eastern part of the field. The western part of the field is dominated by segmented NW-SE faults and NE-SW cross-faults systems (Edwards et al., 2005). The presence of faults and fractures in the reservoirs can have a significant impact on the recovery of hydrocarbon, as they affect the elastic properties of rocks such as porosity and permeability.

The survey was deployed on the southeastern part of the field. The acquisition geometry consisted of spiral source patterns centered at the wellhead with a maximum offset of 3000 m. The spiral arms were spaced every 50 m in the radial direction. 18364 shots spaced every 25 m and 70 receivers spaced every 20 m in the deviated borehole were used (Figure 1). The shallowest receiver was located at 1145 m depth. The seismic data were reverse time migrated and a high-resolution seismic image (Figure 2), with a radial extension of around 1000 m from the wellhead was obtained.

We used the migrated section to extract faults and fractures following a specific workflow and provide an estimate of the fracture intensity map. The term fracture here also refers to fracture corridors, i.e. zones containing closely spaced fractures.

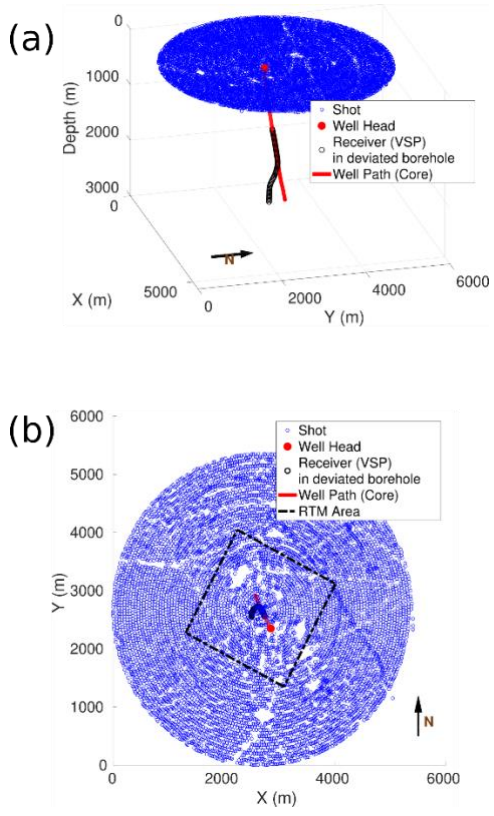

Figure 1. 3D VSP acquisition geometry (a), and plan view (b). RTM area in (b) refers to reverse time migration.

METHOD AND RESULTS

The workflow for the extraction of faults and fractures is explained in details in (Takam Takougang et al., 2018, 2019). The workflow was applied with success using 2D walkaway seismic data (Takam Takougang et al., 2019) and expanded to 3D (Takam Takougang et al., 2018). Here we provide an overview of the method.

In essence, the methodology consists of:

1. Preconditioning the input data which consist in this case in the removal of acquisition footprint in the wavenumber domain using a modified Gaussian function.
2. Automatic extraction of faults and fractures using a semblance based discontinuity attribute (Hale, 2013). The attribute provides the maximum likelihood of point being part of a fault or discontinuity surface.
3. Binary filtering and thinning for the enhancement of the results
4. Clustering to discriminate fractures and small scale faults from large scale faults, and also remove structures likely related to noise. The success of clustering depends on available a priori structural geological information

We present the results at 3 reservoir zones (R1, R2, R3), and access their reliability by comparing their strike directions to those from fractures interpreted from core and FMI data.

Faults and Fractures at reservoir zones

Figures 3, 4, and 5 show the extracted lineaments at reservoirs R1, R2, and R3 respectively. It appears that the lineaments are orientated in various directions with the dominant strike directions orientated NNE-SSW in reservoir R1 and NNW-SSE in reservoirs R2 and R3. These orientations are in good agreement with dominant strike directions of interpreted fractures from FMI and core data (Figures 3, 4, and 5); thus giving confidence that the lineaments are related to fractures or fracture corridors. In addition, a known segmented fault (flower structure) orientated WNW-ESE to NW-SE was detected and isolated from the rest of the lineaments through clustering. The fault is highlighted in magenta in Figures 3, 4 and 5.

Fracture intensity maps

We used the extracted fracture network to calculate fracture intensity maps. Fracture intensity maps are used to estimate zones with high and low fracturing. We used the circular scan method of Mauldon et al. (2001) to estimate the intensity map at every selected depth slide. In this method, intersections of fractures in a number of selected scan circles are used to estimate the fracture intensity. The intensity map *I* for a single scan circle can be express as:

$$I = \frac{n}{4r}$$

where n represents the number of fractures' intersections with the circle, and r the circle radius (m). The intensity map of a 2D depth slide is estimated by averaging the fracture intensity *I* for each scan circle.

Figure 6 shows the intensity map for six increasing depth slices, S1, R1, R2, R3, S2 and S3 (See Figure 2 for location). Zones with relatively intense fracturing are generally located north to north-west of the well. Deeper, at S2 and S3, these zones can also be found west and south of the well. Zones with intense fracturing are generally associated with more fractures' intersections and connectivity, which affect the reservoir porosity and permeability.

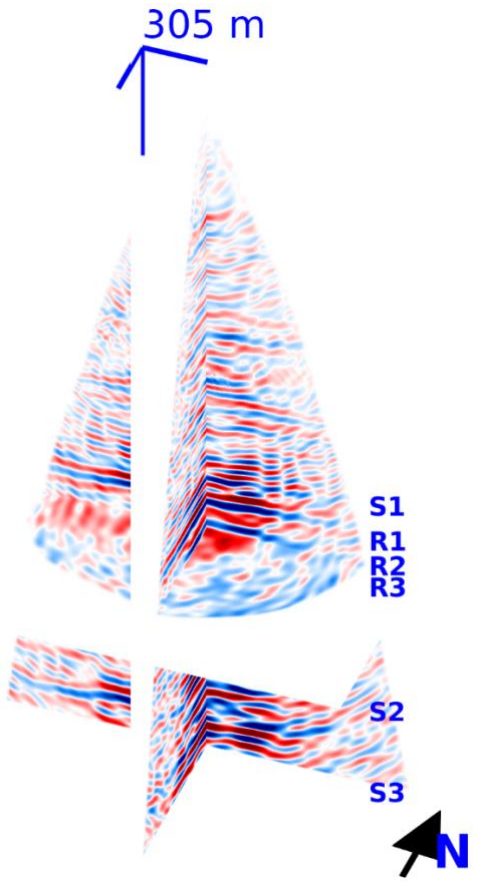

Figure 2. Reverse time migrated cube. R1, R2, and R3 are reservoir intervals and S1, S2 and S3 are selected slices used for fracture intensity map interpretation.

CONCLUSIONS

We have used a workflow to extract faults and fractures from 3D VSP data acquired in a carbonate reservoir offshore Abu Dhabi in the United Arab Emirates. The Strike directions of the extracted fractures show good correlation with interpreted fractures from FMI and core data. Two dominants strike directions were obtained: NNE-SSW and NNW-SSE. A known segmented fault in the area orientated WNW-ESE to NW-SE was also detected. Computed fracture intensity maps suggest that zones with relatively intense fracturing are located north to north-west of the well. Deeper, zones with intense fracturing can also be found west and south of the well. These zones are potentially characterized by relatively greater porosity and permeability.

ACKNOWLEDGMENTS

We are grateful to Abu Dhabi National Oil Company (ADNOC) for sponsoring this project and providing the data. Special thanks to dGB Earth Sciences for providing their software.

REFERENCES

Alsharhan, A.S., 1989, Petroleum geology of the United Arab Emirates, Journal of Petroleum Geology, 12, 253-288.

Edwards, E., Alrougha, H.B., Sit, A., Sultan, A., and Khouri, N., 2005, Resolution of a multi-set, strike-slip dominated fault system, identified from 3D seismic, in early Cretaceous carbonate reservoir sequences of a giant offshore field in Abu Dhabi, Society of Petroleum Engineers SPE 93489, 1-16.

Hale, D., 2013, Methods to compute fault images, extract fault surfaces, and estimate fault throws from 3D seismic images, Geophysics, 78, 033-043.

Hassan, T., and Wada, Y., 1981, Geology and Development of Thamama Zone 4, Zakum Field, Society of Petroleum Engineers SPE-7779-PA, 1327-1337.

Mauldon, M., Dunne, W., and Rohrbaugh, M., 2001, Circular scanlines and circular windows: new tools for characterizing the geometry of fracture traces, Journal of Structural Geology 23, 247-258.

Takam Takougang, E. M., Ali, M. Y., and Bouzidi, Y., 2018, Mapping faults and fractures in a carbonate reservoir from 3D VSP data, SEG Technical Program Expanded Abstracts, 5397-5401.

Takam Takougang, E.M., Bouzidi, Y., and Ali, M.Y., 2019, Characterization of small faults and fractures in a carbonate reservoir using waveform inversion, reverse time migration, and seismic attributes, Journal of Applied Geophysics, 161, 116 -123.

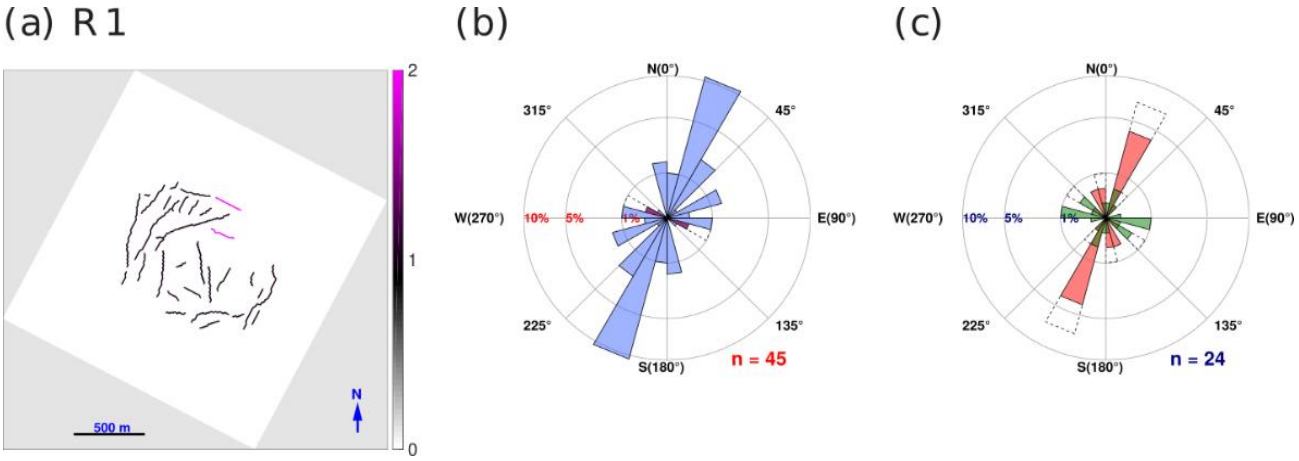

Figure 3. (a) Extracted fractures in reservoir R1, and (b) associated rose diagram. The isolated faults in (a) and their contribution to the rose diagram in (b) are indicated in magenta. (c) Rose diagram of interpreted fractures from core data in reservoir R1; the closed fractures are shown in light red and the open fractures in green. The doted petals represent the orientation of combined lineaments of various nature (faults and fractures in (b), open and closed fractures in (c). n is the number of counts.

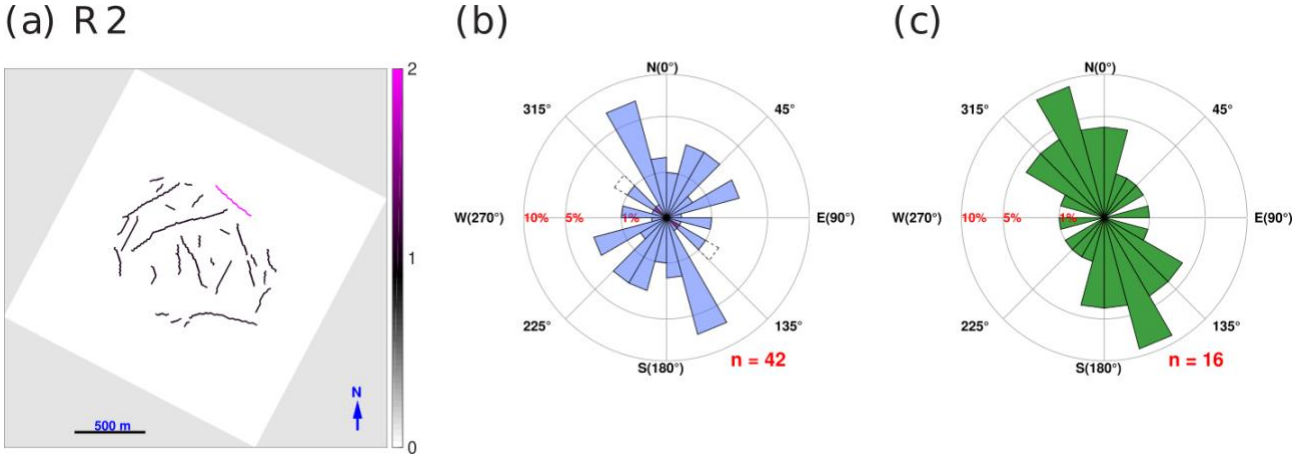

Figure 4. (a) Extracted fractures in reservoir R2, and (b) associated rose diagram. The fault in (a) and its contribution to the rose diagram in (b) are indicated in magenta. (c) Rose diagram of interpreted open fractures from FMI data in reservoir R2. The doted petals in (b) represent the orientation of combined lineaments (faults and fractures). n is the number of counts.

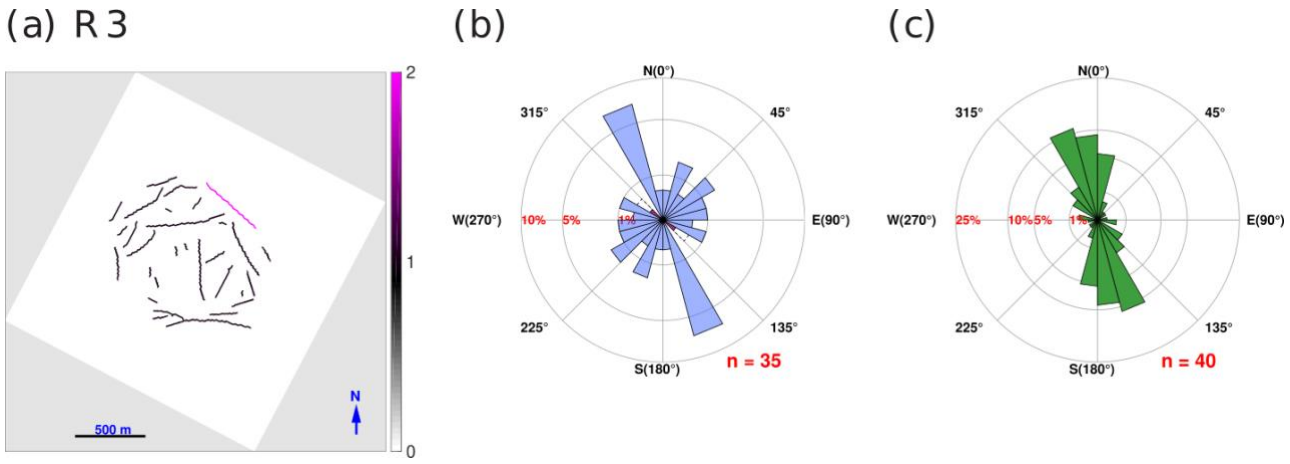

Figure 5. (a) Extracted fractures in reservoir R3, and (b) associated rose diagram. The isolated fault in (a) and its contribution to the rose diagram in (b) is indicated in magenta. (c) Rose diagram of interpreted open fractures from FMI data in reservoir R3. The doted petals in (b) represent the orientation of combined lineaments (faults and fractures). n is the number of counts.

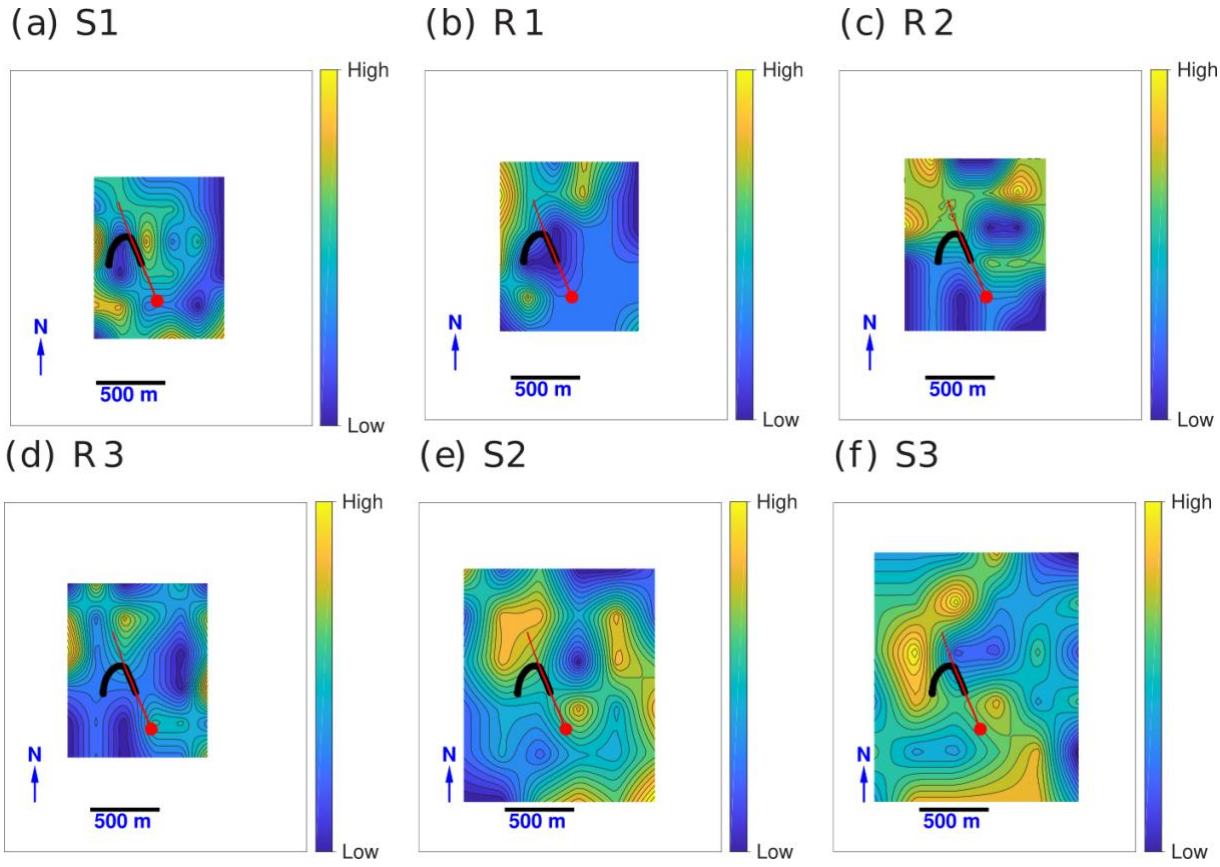

Figure 6. Estimated Fracture intensity maps at six increasing depth slices, S1, R1, R2, R3, S2, S3 (see Figure 2 for locations). The red circle indicates the location of the wellhead. The red line shows the trajectory of the well path, and the black circles the VSP receivers.